

# On Calcium Carbonates: from Fundamental Research to Application\*

Ljerka Brečević\*\* and Damir Kralj\*\*

*Laboratory for Precipitation Processes, Ruđer Bošković Institute, P.O. Box 180, HR-10002 Zagreb, Croatia*

RECEIVED JANUARY 8, 2007; ACCEPTED MAY 17, 2007

*Keywords*  
Calcium carbonates  
calcite  
vaterite  
amorphous calcium carbonate  
calcium carbonate hexahydrate  
calcium carbonate monohydrate  
elementary precipitation processes  
mechanisms  
kinetics

Appearance of a solid phase from aqueous solution, known as precipitation, is responsible for the formation of numerous natural materials and technological products. Therefore, the knowledge on mechanisms of elementary processes involved in precipitation should be considered in the areas such as geology, oceanology, biomineralization, medicine, basic chemical and pharmaceutical industries, analytical and materials chemistry in particular. Calcium carbonates are a very suitable model system for investigations of these processes. Owing to their low solubility, a wide range of initial supersaturations can be achieved that direct to different conditions under which a particular process dominates. Calcium carbonates can precipitate in the form of six modifications (polymorphic or hydrated). In the Laboratory for Precipitation Processes, systematic investigations of the conditions for formation, crystal growth and transformation of amorphous calcium carbonate, calcium carbonate hexahydrate, calcium carbonate monohydrate, vaterite and calcite have been performed during the last nearly twenty years. An overview of these studies is presented.

## INTRODUCTION

Precipitation of a solute from its homogeneous solution is one of the possible ways by which a substance is transformed from one (liquid) phase into another (solid). According to one of the definitions,<sup>1</sup> precipitation from solution is regarded as a fast crystallization. Since the speed of crystallization is proportional to supersaturation, it can be considered that precipitation starts at high supersaturations. Only relatively insoluble substances develop high supersaturations, so that precipitation can also be considered the crystallization of sparingly soluble substances.

A number of processes are involved in precipitation and these are shown in Figure 1.<sup>2</sup> Precipitation starts with

a nucleation process (homogeneous or heterogeneous) in a supersaturated solution. Nucleation is often energetically the most difficult process in the sequence of precipitation events, because this step will start only if the energy barrier associated with the extra surface energy (change of the Gibbs energy) of the clusters (nuclei) formation is overcome. Nuclei form either as spontaneous associates (embryos, homogeneous nuclei) of growth units (molecules, ions or atoms) from the solution or by using the surface of a foreign solid phase (impurity particles) already present in the solution (heteronuclei). The dimensions of nuclei are negligible (typically less than 100 growth units) and the consumption of substance from the solution during nucleation is rather small. The nuclei formed grow into crystallites, with an occasional parallel

\* Dedicated to Professor Nikola Kallay on the occasion of his 65<sup>th</sup> birthday.

\*\* Author to whom correspondence should be addressed. (E-mail: brecevic@irb.hr; kralj@irb.hr)

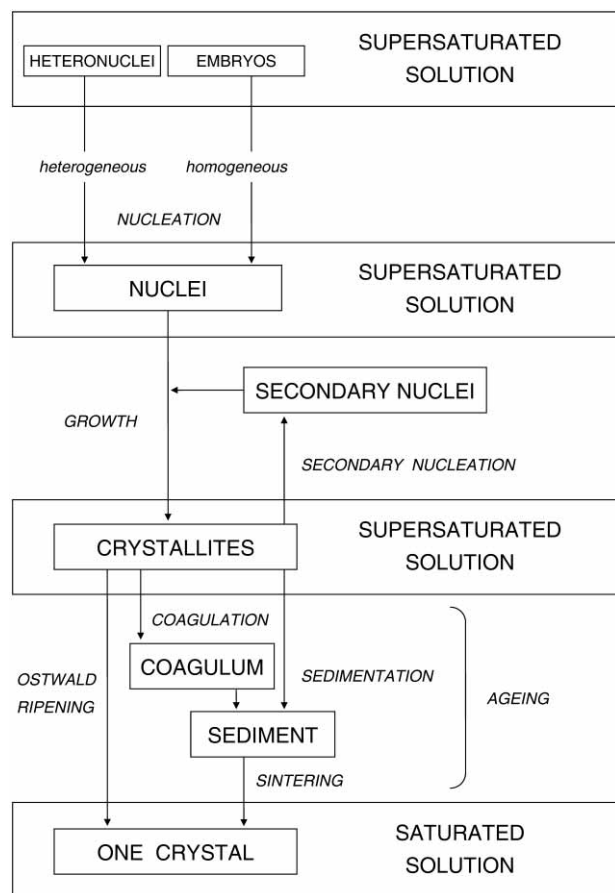


Figure 1. Stages and pathways of precipitation processes (after Ref. 2).

formation of secondary nuclei (initiated by the presence of the crystallizing solid phase itself). This process, known as crystal growth, is accompanied by the most significant changes in the solution concentration of the precipitating phase. Crystal growth itself is a complex process which may be considered to occur in two main groups of elementary processes that take place either at some distance from the crystal surface or at the crystal-solution interface. These elementary processes are, respectively, diffusion and/or convection of growth units through the bulk of solution toward the crystal-solution interface, and surface integration processes at the crystal-solution interface. The slowest of these consecutive processes becomes the rate-determining of the overall crystal growth rate.<sup>1-3</sup> The solid phase thus formed (crystals) undergoes further changes in physical and/or chemical properties. These secondary changes occur under conditions close to equilibrium and are the consequence of the tendency of the precipitation system to establish equilibrium. Theoretically, precipitation terminates when the crystals present in the system form one crystal in equilibrium with the saturated solution. In practice, precipitation is completed when crystals reach a size that causes sedimentation. The process that leads to equilibrium is called ageing and takes

place through several possible ways. Ostwald ripening (dissolution of small and simultaneous growth of large particles) and recrystallization are the mechanisms that probably always occur in the early stages of the precipitate formation. Coagulation and agglomeration, followed by sintering, change the initial dispersion of the system by formation of more stable large aggregates. Unstable and metastable solid phases, which often precipitate initially, transform into thermodynamically stable modifications. These metastable phases (polymorphs, hydrates or amorphous substances) have various thermodynamic stabilities that manifest itself as a difference in solubility at given conditions. The phenomenon was recognized and formulated by Ostwald<sup>4</sup> as his Law of Stages. According to this law, the least stable phase, having the highest solubility, precipitates first and subsequently transforms to the more stable one. The transformation occurs either by internal rearrangements of atoms, ions or molecules (solid-state transition)<sup>5-7</sup> or by dissolution of the metastable phase(s) in the solution with which this phase(s) is in contact, and simultaneous precipitation of the stable phase from the same solution (solution mediated transformation).<sup>8-12</sup>

Physical-chemical properties (*e.g.* particle size, morphology, chemical and mineralogical composition) of solid (inorganic) materials, produced by precipitation from aqueous solutions, depend on a series of factors. The effect of a particular of these factors is usually more pronounced during one of the precipitation processes (nucleation, crystal growth or ageing). By choosing a larger number of suitable precipitation model systems and by varying experimental conditions and techniques, it is possible to separate and emphasize the action only of one of these processes and eventually gain generic answers about the behaviour of the precipitated materials.

The investigation of precipitation processes in our Laboratory started in 1968, when it was founded at the Ruđer Bošković Institute. Herein we report our own contribution to this field, on the example of calcium carbonate ( $\text{CaCO}_3$ ), the model system chosen primarily for the study of fundamental precipitation processes but also for the study of problems related to calcium carbonate being a commercial material and a constituent in many natural systems.

Calcium carbonate is the most important material for use as a filler and pigment in the production of paper, rubber, plastic, pharmaceuticals, food, paint, textiles and many other materials. It also has a significant impact on energy production and water treatment (scaling) and is widespread in the natural environment (biological systems:<sup>13-15</sup> mollusc shells, egg shells, pearls, corals and exoskeletons of arthropods, calculi, *etc.*; geological systems:<sup>16,17</sup> sedimentary rocks, calcareous travertine). In all these instances, chemical composition and polymorphism, crystal size distribution and morphology of the crystals,

as well as mechanisms involved in biomineralization processes (in which an organic matrix plays an important role in control of the properties of the mineral phase), are of great significance.<sup>18–20</sup> Calcium carbonate is also a suitable model system for the study of formation and growth of metastable phases and their transformation into the stable form(s) because it appears in several different solid modifications, three hydrated forms (calcium carbonate monohydrate, calcium carbonate hexahydrate and amorphous calcium carbonate) and three anhydrous polymorphs (calcite, aragonite and vaterite), among which calcite is the only thermodynamically stable modification under standard conditions. The investigation of the kinetics and mechanisms of the processes involved in the precipitation of calcium carbonate modifications helps to elucidate of the nature and behaviour of metastable phases in general and to comprehend the processes in which the kinetic consideration is of greatest importance. Likewise, the investigation of the influence of foreign ions and molecules (both of inorganic and organic nature) on the kinetics and mechanisms of the precipitation processes, as well as on the mode and sites of their possible incorporation into the calcium carbonate crystal lattice, shed more light upon the mechanisms of biomineralization processes.

## CALCIUM CARBONATES

In order to study the fundamental processes involved in the formation and transformation of calcium carbonates, some properties of the electrolyte solution from which the solid phase precipitates and of the possible metastable and stable solid modifications are necessary to be known. Certainly, the most important thermodynamic parameters that influence the overall precipitation process are the electrolyte supersaturation and the solubility of the solid phase(s) involved.

### *Amorphous Calcium Carbonate*

Amorphous calcium carbonate, which appears as a »precursor« in spontaneous precipitation at relatively high supersaturations, is a rather unstable solid phase, which undergoes a rapid transformation to more stable anhydrous forms. Although an amorphous hydrated calcium carbonate was described in 1938,<sup>21</sup> we characterized such a substance much later.<sup>22</sup> In the preparation of the amorphous substance the precipitation was carried out under controlled conditions (initial reactant concentrations, total volume of the system, temperature, stirring rate) and the precipitate formed was characterized by electron microscopy, thermogravimetry, IR spectroscopy and X-ray diffraction. The precipitate consisted of spherical particles with the diameter in the range from 50 to 400 nm (Figure 2) and contained less than 1 molecule of water per molecule of  $\text{CaCO}_3$ . This water was evidently located at dif-

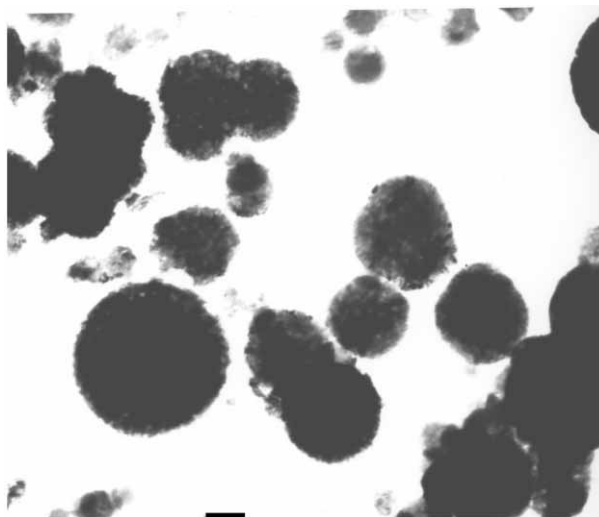


Figure 2. Electron micrograph of the spherical calcium carbonate particles which are amorphous with respect to IR spectroscopy and X-ray diffraction. Bar = 100  $\mu\text{m}$ .

ferent positions inside the substance structure and was differently bonded. Depending on the way of bonding (zeolitic or crystalline lattice water) or just entrapping during the very rapid formation of the particles, a part of water was released at approximately 200 °C and the rest was released gradually in the interval from about 100 °C to about 500 °C. The existence of bonded water was also confirmed by IR spectroscopy. The infrared spectrum of the amorphous calcium carbonate was studied in more detail in the region from 4000 to 400  $\text{cm}^{-1}$  and at the temperature of liquid nitrogen,<sup>23</sup> the temperature to which the substance was freeze-dried immediately after preparation and kept subsequently, to prevent its transformation into more stable crystalline polymorphs. Normal vibration frequencies of the carbonate ion in the amorphous form ( $\nu_1 = 1067 \text{ cm}^{-1}$ ,  $\nu_2 = 864 \text{ cm}^{-1}$ ,  $\nu_{3a} = 1490 \text{ cm}^{-1}$ ,  $\nu_{3b} = 1425 \text{ cm}^{-1}$ ,  $\nu_{4a} = 725 \text{ cm}^{-1}$  and  $\nu_{4b} = 690 \text{ cm}^{-1}$ ) were explained and also compared with those in the three crystalline polymorphs. The broad bands of the spectrum obtained refer to a poorly crystalline material, which was also confirmed by X-ray diffraction analysis, by which no reflections characteristic of the crystalline material was observed.

The solubility of the amorphous calcium carbonate was determined in the same experimental set-up in which the precipitate was prepared. Freshly deionized water was then added rapidly (within 30 s) into the system continuously stirred, until the background turbidity (clear solution) was obtained again. The flow rate of the water added from an automatic burette was calibrated so that the volume of water could be calculated. The changes in turbidity were followed by means of a photodetector illuminating through the system, and the signal was automatically recorded as a function of time. The solubility was calculated as the stoichiometric concentration of

$\text{CaCO}_3$  in the solution at the moment when the system became clear. It was possible to apply this method because the amorphous phase dissolves rapidly when it finds itself in an undersaturated solution and because the more stable crystalline phases form relatively slowly although the system is much higher supersaturated with respect to calcite, aragonite and vaterite than to the unstable amorphous phase.

The thermodynamic equilibrium constant of dissolution (solubility product) in aqueous solutions of the amorphous calcium carbonate,  $K_s^\circ(\text{amorph})$ , was determined in the temperature range from 10 to 50 °C and the solubility,  $c_s$ , was found to be higher than the solubilities of other calcium carbonate modifications (Table I).

#### Calcium Carbonate Hexahydrate, $\text{CaCO}_3 \cdot 6\text{H}_2\text{O}$

Two hydrated crystalline forms of calcium carbonate, calcium carbonate hexahydrate and calcium carbonate monohydrate, are somewhat more stable compared with amorphous calcium carbonate. These modifications can be kept unchanged for a few days at temperatures below 0 °C before they undergo transformation into calcite. Generally, hydrated forms often precipitate from supersaturated solutions before the more stable anhydrous forms, so the knowledge of their properties is necessary.

Calcium carbonate hexahydrate was first prepared and described as far back as the nineteenth century,<sup>24,25</sup> but its crystallographic properties,<sup>26</sup> density<sup>27</sup> and crystal structure<sup>28</sup> were not reported until the twentieth century.

In order to determine its solubility, we prepared  $\text{CaCO}_3 \cdot 6\text{H}_2\text{O}$  and characterized it by means of optical microscopy, IR spectroscopy and thermogravimetry.<sup>29</sup> Because of its instability at room temperature, all reactant solutions were cooled to less than -10 °C and the synthesis was performed in a refrigerated room kept at 5 °C. Calcium carbonate hexahydrate crystallized in well-defined rhombohedral crystals in the size range 10–40 µm (Figure 3), which were found to decompose at the temperatures above 6 °C. Therefore, the crystals were kept in a freezer at -15 °C.

According to the thermogravimetric analysis, calcium carbonate hexahydrate started to lose mass (water) at about 40 °C and continued up to 300 °C. Nearly all the water was released at about 140 °C and the peak temperature was found to be 125 °C (at a heating rate of 10

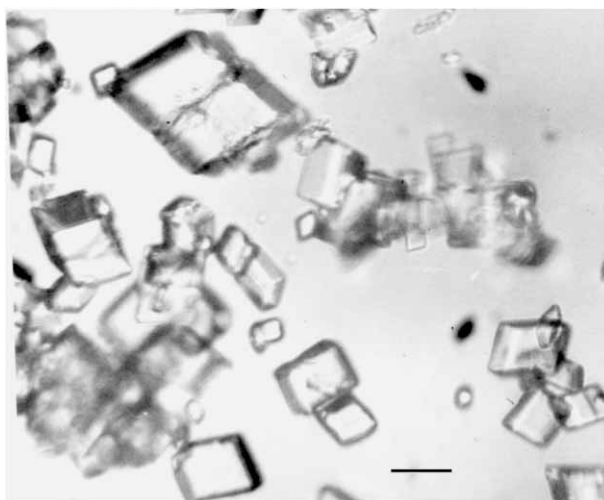


Figure 3. Micrograph of the calcium carbonate hexahydrate crystals. Bar = 20 µm.

°C/min). The total loss of mass corresponded to 5.9–6 molecules of water per molecule of calcium carbonate.

IR spectra were recorded in the region from 4000 to 200  $\text{cm}^{-1}$ . Special precaution was taken to avoid a possible decomposition of the crystals and cooling at the temperature of liquid nitrogen was necessary in order to prevent a loss of lattice water during the analysis. The part of spectrum in the region from 1800 to 200  $\text{cm}^{-1}$  was recorded at room temperature using KBr (1800–600  $\text{cm}^{-1}$ ) and CsI (450–200  $\text{cm}^{-1}$ ) pellets. The absorption bands appear in the regions characteristic of hydrated calcium carbonate modifications.<sup>23,30</sup> It was found that the water molecule vibration in the region from 3500 to 3000  $\text{cm}^{-1}$  was composed of at least three bands, the part of the spectrum from 1700 to 1500  $\text{cm}^{-1}$  corresponding to the normal vibrations of the carbonate ion. Although the carbonate ion bands showed some similarities to the bands of unhydrated modification vaterite,<sup>23,31</sup> the lattice vibrations (450–200  $\text{cm}^{-1}$ ) were completely different.

The solubility of calcium carbonate hexahydrate was determined in the temperature interval from 10 to 40 °C by recording pH during the hexahydrate dissolution in water (entrance of carbon dioxide was prevented). The pH value at the solubility equilibrium, obtained by dissolving different amounts of the substance in water at the predetermined temperature until the final constant pH value was reached, was used for the calculation of calcium carbonate hexahydrate solubility product (or equilibrium constant):

$$K_s^\circ(\text{CaCO}_3 \cdot 6\text{H}_2\text{O}) = a(\text{Ca}^{2+})_{\text{eq}} \cdot a(\text{CO}_3^{2-})_{\text{eq}} \quad (1)$$

In calculating the activities, seven ionic species were assumed to be present in solution at significant concentrations ( $\text{Ca}^{2+}$ ,  $\text{CaCO}_3^\circ$ ,  $\text{CaHCO}_3^+$ ,  $\text{CO}_3^{2-}$ ,  $\text{HCO}_3^-$ ,  $\text{H}^+$ ,  $\text{OH}^-$ ).

TABLE I. Solubility of amorphous calcium carbonate

| $\theta / ^\circ\text{C}$ | $c_s / \text{mmol dm}^{-3}$ | $-\lg K_s^\circ$ | Standard error |
|---------------------------|-----------------------------|------------------|----------------|
| 10.0                      | 1.84                        | 6.266            | 0.009          |
| 25.0                      | 1.70                        | 6.393            | 0.015          |
| 40.0                      | 1.53                        | 6.594            | 0.011          |
| 55.0                      | 1.40                        | 6.822            | –              |



TABLE II. Solubility of calcium carbonate hexahydrate

| $\theta / ^\circ\text{C}$ | $c_s / \text{mmol dm}^{-3}$ | $-\lg K_s^\circ$ | Standard error |
|---------------------------|-----------------------------|------------------|----------------|
| 10.0                      | 0.43                        | 7.245            | 0.001          |
| 25.0                      | 0.37                        | 7.461            | 0.005          |
| 40.0                      | 0.34                        | 7.711            | 0.005          |

The solubility was calculated on the basis of the following balance equation:

$$c_s = c(\text{Ca}^{2+}) + c(\text{CaCO}_3^\circ) + c(\text{CaHCO}_3^+) = c(\text{CO}_3^{2-}) + c(\text{HCO}_3^-) + c(\text{CaCO}_3^\circ) + c(\text{CaHCO}_3^+) \quad (2)$$

The results are given in Table II. The solubility was found to be higher than those of calcite, aragonite and vaterite,<sup>32</sup> and lower than that of amorphous calcium carbonate.

#### Calcium Carbonate Monohydrate, $\text{CaCO}_3 \cdot \text{H}_2\text{O}$

The first information on calcium carbonate monohydrate was given in 1930.<sup>33</sup> Later on it was reported on its existence as a mineral (monohydrocalcite), mainly as a constituent in lake sediments.<sup>34,35</sup> According to the reports on syntheses,<sup>35–38</sup> it is obvious that an important part in the preparation of calcium carbonate monohydrate and in natural occurrence is due to the presence of magnesium, some other seawater constituent ions, organic material and microorganisms. There is also evidence for the powder diffraction<sup>34,35,39,40</sup> and crystallographic data,<sup>41,42</sup> as well as the crystal structure<sup>30</sup> of various natural and synthetic calcium carbonate monohydrates. IR spectra of some of these substances<sup>30,42</sup> and the solubility measurements in water at 25 °C of a natural specimen<sup>40</sup> were reported. This last paper also gives the free energy of formation and a standard enthalpy estimation of the specimen. Not long ago, calcium carbonate monohydrate became the subject of the electron paramagnetic resonance (EPR) studies of the radiation effect on calcium carbonates.<sup>43</sup> Since then, some of its isotropic signals have frequently been used for dating natural carbonates.

In continuation of our studies of metastable calcium carbonate modifications, the dissolution kinetics and the solubility of a synthetic calcium carbonate monohydrate in pure water and in a temperature range from 15 to 50 °C was investigated.<sup>44</sup> Such investigations were undertaken because of an important problem that arose from dissolution of calcium carbonates in natural waters and also because of the lack of solubility data at different temperatures.

Calcium carbonate monohydrate,  $\text{CaCO}_3 \cdot \text{H}_2\text{O}$ , used in the experiments was prepared after the slightly modified method of Duedall and Buckley.<sup>45</sup> In order to characterize the crystals, light microscopy, thermogravimetry, FT-IR spectroscopy and X-ray diffractometry were appli-

ed. Calcium carbonate monohydrate, the hexagonal modification of hydrated calcium carbonates, crystallized in well-defined spherical crystals with diameters between 15 and 30  $\mu\text{m}$  (Figure 4). Thermogravimetric analysis showed that a mass loss of 15.25 % started at about 150 °C and continued until 274 °C, the peak temperature being 188 °C at the heating rate of 10 °C/min. FT-IR spectra and X-ray diffraction patterns showed no other absorption bands and diffraction lines than those of calcium carbonate monohydrate,<sup>30,46</sup> thus confirming the purity of the substance.

Solubility was determined by recording pH of the solution during the dissolution of the monohydrate crystals in water, preventing any exchange of carbon dioxide between the air and the solution. The solubility product,  $\text{p}K_s^\circ$ , was calculated from the pH values measured at the solubility equilibrium (maximum pH) taking into account all the relevant calcium and carbonate species. The results obtained are summarized in Table III. Up to the time these results were published, the only  $\text{p}K_s^\circ$  value found in the literature was  $\text{p}K_s^\circ = 7.60 \pm 0.03$  determined at 25 °C.<sup>40</sup> The difference between this value and the values given in Table III could be ascribed to the fact that a natural specimen, usually containing different admixtures, was probably used in that investigation. In any case, calcium carbonate monohydrate was found to be more soluble than anhydrous polymorphs.<sup>32</sup>

The dissolution kinetic experiments were performed at 15, 25, 35 and 45 °C and the amount of crystals added was such that after reaching the equilibrium, an amount of undissolved crystals was still present in the system. Among the theoretical models tested, a second-order surface-controlled process was found to describe best the mechanism of the dissolution process. The values for

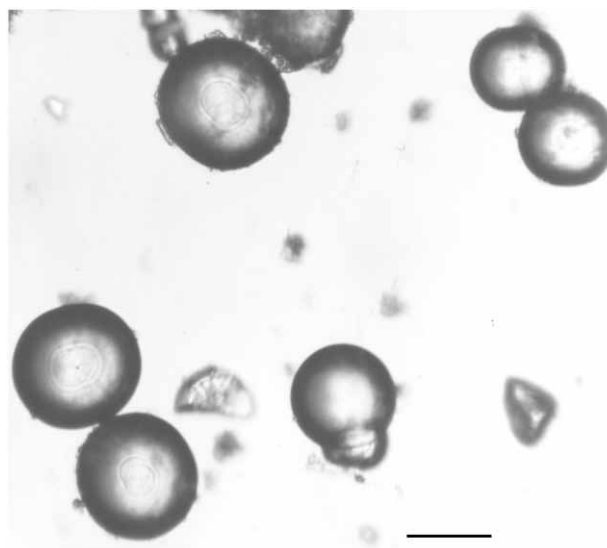


Figure 4. Micrograph of the calcium carbonate monohydrate spherical particles. Bar = 20  $\mu\text{m}$ .

TABLE III. Values of calcium carbonate monohydrate solubility product

| $\theta / ^\circ\text{C}$ | $-\lg K_s^\circ$ |
|---------------------------|------------------|
| 15.0                      | 7.0636           |
| 15.0                      | 7.0734           |
| 25.0                      | 7.2120           |
| 25.0                      | 7.1772           |
| 35.0                      | 7.2129           |
| 35.0                      | 7.2155           |
| 35.0                      | 7.2199           |
| 45.0                      | 7.3460           |
| 45.0                      | 7.3662           |
| 50.0                      | 7.4441           |
| 50.0                      | 7.4890           |

the dissolution rate constants,  $k$ , obtained at different temperatures, and the absolute temperature of the dissolution experiments,  $T$ , plotted according to the Arrhenius plot,  $\ln k$  vs.  $1/T$ , enabled us to calculate of the activation energy for dissolution of calcium carbonate monohydrate,  $E_a = 73.3 \pm 6.8$  kJ/mol. This, relatively high activation energy is in support of the proposed mechanism.

#### Vaterite, $\text{CaCO}_3$

Vaterite is the least stable of the calcium carbonate anhydrous modifications under standard conditions and transforms easily and irreversibly into one of the two thermodynamically more stable forms (aragonite, calcite) when in contact with water. Because of its instability, vaterite is not as wide spread in nature as the other polymorphs are. Yet, owing to the particular conditions, which stabilized vaterite, preventing its transformation into aragonite or calcite, it was found in sediments,<sup>47</sup> metamorphic rocks,<sup>48</sup> gallstones,<sup>49</sup> fish otoliths and mollusc shells.<sup>50</sup>

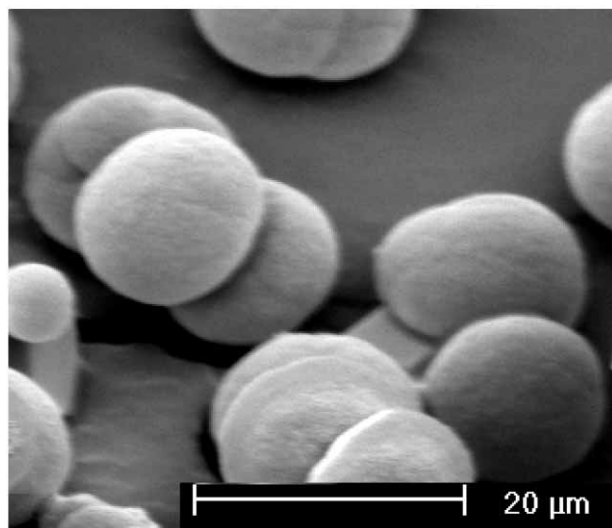


Figure 5. Scanning electron micrographs of vaterite crystals.

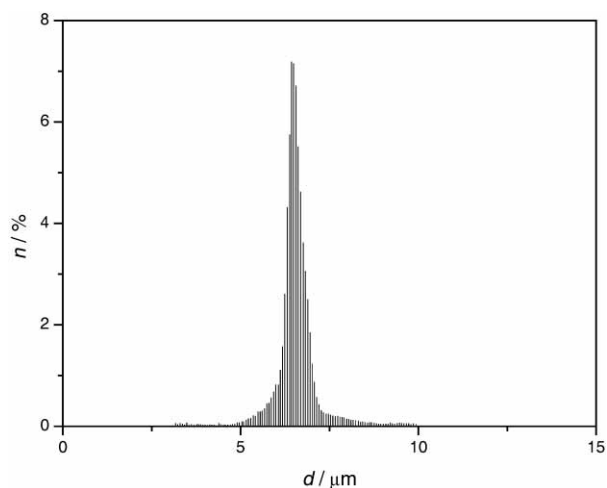


Figure 6. Size distribution of vaterite crystals given as a histogram of 128 size classes.

Besides, there are reports on vaterite being the first solid phase in many spontaneously formed calcium carbonate precipitates<sup>39</sup> and in scale formation,<sup>51</sup> in particular. There are also suggestions<sup>47,52</sup> that vaterite has been acting as a precursor phase in the formation of calcium carbonate geological sediments. In support to this presumption are the experimental observations that the unstable phases of calcium carbonate precipitate first from medium and high supersaturated solutions.<sup>1-3,22,51</sup> For an additional study of these processes and to perceive the nature of calcium carbonate transformations in contact with aqueous solutions, detailed knowledge about the kinetics and mechanisms of dissolution and precipitation processes involved was necessary.

Therefore, we started with gaining knowledge on the conditions for vaterite appearance. It was followed by investigations of the kinetics and mechanisms of its crystal growth and dissolution, which was a basis for the kinetic study of vaterite transformation. All this research was also important in comprehending the processes in which kinetic considerations are essential.

**Preparation.** – It is difficult to obtain pure vaterite by spontaneous precipitation.<sup>53,54</sup> Some authors even claim that it could be obtained at sustained supersaturations only.<sup>55</sup> More frequently vaterite appears in a mixture with aragonite or calcite, which makes it difficult to study the kinetics of crystal growth, dissolution and transformation processes. Therefore, it was essential to develop a reproducible and simple method by which precipitate would consist entirely of vaterite.<sup>56,57</sup> By the proposed method, vaterite particles were obtained in a very narrow region of initial reactant (calcium chloride and sodium carbonate) concentrations ( $c(\text{Ca}^{2+}_{\text{tot}}) = c(\text{CO}_3^{2-}_{\text{tot}}) = 2.5 \times 10^{-3}$  mol  $\text{dm}^{-3}$ ). At that, the initial pH of the reactant solutions had to be between pH = 9.3 and pH = 9.9. The purity of the precipitate was confirmed by X-ray diffrac-

tion and IR spectroscopy, showing that no traces of calcite were present. Observation by scanning electron microscopy demonstrated that vaterite particles were spherulites with an average diameter of about 3.2  $\mu\text{m}$  (Figure 5). A very high monodispersity of these particles was obtained when the precipitation (nucleation) was initiated by ultrasonic irradiation,<sup>57</sup> using a homogenizer equipped with a microtip (see Figure 6).

*Kinetics of Crystal Growth.* – The kinetics of vaterite precipitation from aqueous solution was determined in a temperature range from about 10 to 45  $^{\circ}\text{C}$  and at ionic strengths from 15 to 315  $\text{mmol dm}^{-3}$ .<sup>56</sup> Spontaneous precipitation of pure vaterite was brought about as described above. During the experiments the average particle diameter increased gradually up to a final value of approximately 3.2  $\mu\text{m}$ . The number of particles was of the order of  $10^7$  per  $\text{cm}^3$ , which is a typical value for heterogeneously formed precipitate, and did not increase strongly within the inherently limited range of initial supersaturations. In order to prove this assumption, we compared the value of interfacial tension,  $\sigma$ , which we calculated by assuming that vaterite precipitated by means of homogeneous nucleation followed by mononuclear growth<sup>58</sup> ( $\sigma = 34 \text{ mJ/m}^2$ ), with the value estimated from the general correlation between interfacial tension and the solubility, Eq. (65) in Ref. 59, ( $\sigma = 90 \text{ mJ/m}^2$ ). Thus, the hypothesis on vaterite precipitation being initiated by heterogeneous nucleation was confirmed.

The induction period was observed in experiments performed at low temperature (10  $^{\circ}\text{C}$ ) and in those made at different ionic strengths. In all other cases, the precipitate appeared apparently immediately after mixing the reactants.

After the induction period, the changes of reactant concentrations were assumed to be the consequence of the vaterite crystal growth only. Therefore, the data of pH recorded as a function of time were analysed by means of a computer program. In the first step, the program calculated the concentrations and activities of chosen ionic species by considering the respective protolytic and other ionic equilibria. The equilibrium constants as well as the solubility products for vaterite used were taken from the paper by Plummer and Busenberg.<sup>32</sup> The activity coefficients,  $\gamma_z$ , were estimated by means of the Davies equation,<sup>60</sup> and the Debye-Hückel constant,  $A$ , at different temperatures was calculated by means of an interpolation formula based on a table in Robinson and Stokes' book.<sup>61</sup> The amount of precipitate and the average volume of particles were found from the experimental data of the initial total concentrations and from the measured number of particles. In the second step, the computer program calculated the crystal growth rate,  $dr/dt$ , determined by numerical differentiation, and the saturation ratio,  $S \equiv (a(\text{Ca}^{2+}) \cdot a(\text{CO}_3^{2-}) / K_s^{\circ})^{1/2}$ .

The growth kinetics was found to be parabolic,

$$dr/dt = k_{\text{gv}} (S - 1)^2 \quad (3)$$

the rate constants being  $k_{\text{gv}} = 0.180, 0.468, 0.560, 1.250$  and  $1.860 \text{ nm/s}$  at 11.4, 21.7, 25.0, 33.8 and 42.5  $^{\circ}\text{C}$ , respectively.

Surprisingly, a rather weak dependence of the vaterite growth rate on the ionic strength was found (Figure 7). The values of the rate constants in these experiments at 25  $^{\circ}\text{C}$  were  $k_{\text{gv}} = 0.560, 0.588, 0.594$  and  $0.610 \text{ nm/s}$  at the ionic strengths 15, 65, 115 and 315  $\text{mmol/dm}^{-3}$ , respectively, which could be represented by the equation

$$\lg(k_{\text{gv}}/\text{nm s}^{-1}) = -0.275 + 0.228 [\sqrt{I}/\text{mol dm}^{-3} / (1 + \sqrt{I}/\text{mol dm}^{-3}) - 0.3 I/\text{mol dm}^{-3}] \quad (4)$$

Since we have found no literature data on the activation energy,  $E_a$ , for the crystal growth of vaterite, the change of the rate constants with temperature, according to the Arrhenius plot, was determined. The value calculated from the slope of the straight line obtained,  $E_a = 57.1 \text{ kJ/mol}$ , supported the surface reaction controlled mechanism. However, it was shown that the rate constants found were in quantitative agreement with those calculated from the theory of electrolyte crystal growth,<sup>59,62</sup> which means that the rate-determining mechanism in the growth process was the dehydration of calcium ions at the moment when they integrate in the growth sites.

*Kinetics of Dissolution.* – Generally, the dissolution process takes place in two steps: (i) reaction at the crystal surface, which involves disintegration of the crystal lattice,

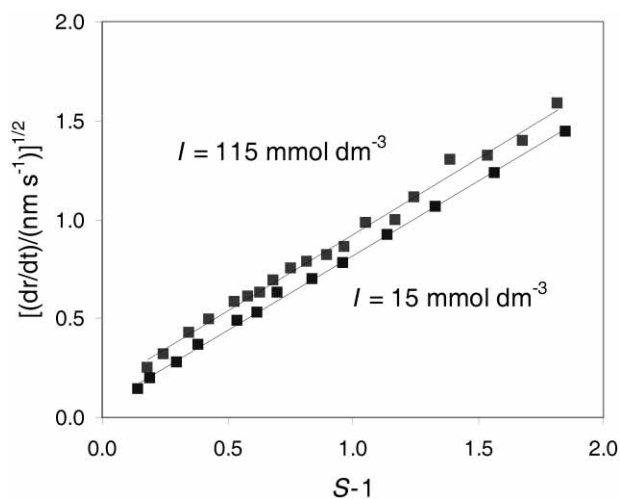


Figure 7. Plots of the square root of the growth rate,  $(dr/dt)^{1/2}$ , as a function of the relative supersaturation,  $S - 1$ , for 25  $^{\circ}\text{C}$  and various ionic strengths.

hydration of the lattice ions and possibly their diffusion over a distance in an ion adsorption layer on the crystal surface, and (ii) transport of thus dissolved matter away from the crystal surface or the interface region through the bulk solution, which may take place by diffusion and/or convection.

Our investigations of the vaterite dissolution kinetics in aqueous solutions were performed in two sets of experiments, in which either the influence of temperature (15 to 45 °C) or the effect of ionic strength (50 to 200 mmol dm<sup>-3</sup>) were studied.<sup>57</sup> The vaterite crystals used were highly monodispersed (2.7 to 4.6 μm), prepared as described above by means of the ultrasonication method. The progress of the dissolution was followed by monitoring pH as a function of time, from which the concentration of the dissolved vaterite crystals was calculated. These data were used in calculating the radius, *r*, of the spherical vaterite particles and the dissolution rate,  $-dr/dt$ , was determined by numerical differentiation of *r* as a function of time, *t*. Because of very low concentrations of ionic species, liberated by vaterite dissolution, the pH measurements were extremely susceptible to contamination with CO<sub>2</sub> from the atmosphere. Therefore, it was necessary that the CO<sub>2</sub> content in water was determined before each experiment. This value was then used as a correction in calculating the total carbonate concentration present in the system. The experimental system was prevented from any further contact with carbon dioxide from the air.

In both sets of experiments straight lines were obtained when  $-r(dr/dt)$  was plotted as a function of undersaturation,  $c_{sv} - c$ , which, according to the theory, assumes diffusion of the hydrated constituent ions away from the crystal surface into the bulk solution. Therefore, the solubility of vaterite,  $c_{sv}$ , for the given temperatures was calculated as the value of the total calcium ion concentration in a saturated solution.

In order to check the assumption of vaterite dissolution rate being controlled by diffusion, apparent diffusion coefficients,  $D_{app}$ , were estimated from the theoretical equation derived from Fick's first law:

$$-dr/dt = D V_m (c_{sv} - c)/r \quad (5)$$

where *D* is the diffusion coefficient,  $V_m$  is the molar volume and  $c_{sv}$  is the solubility. The values for  $D_{app}$  thus obtained were compared with the diffusion coefficients of Ca<sup>2+</sup> ions calculated from electric conductivities,  $D_{cond}$ , by means of the Nernst equation<sup>63</sup> (see Table IV). Although some small discrepancies between  $D_{app}$  and  $D_{cond}$  existed, primarily due to several approximations made in the calculations, the differences were not large enough to disprove the diffusion controlled mechanism of vaterite dissolution. The possible influence of convection on the dissolution rate was negligible since the vaterite par-

TABLE IV. Apparent diffusion coefficients,  $D_{app}$ , calculated from the kinetics of vaterite dissolution in experiments at different temperatures,  $\theta$ , and initial ionic strengths, *I*, and diffusion coefficients,  $D_{cond}$ , calculated by means of Nernst equation

| $\theta / ^\circ\text{C}$ | <i>I</i> /<br>mmol dm <sup>-3</sup> | $10^{10} D_{app} /$<br>m <sup>2</sup> s <sup>-1</sup> | $10^{10} D_{cond} /$<br>m <sup>2</sup> s <sup>-1</sup> | $D_{app} / D_{cond}$ |
|---------------------------|-------------------------------------|---|--|----------------------|
| 15.0                      | 50                                  | 5.11  | 6.05   | 0.845                |
| 25.0                      | 50                                  | 7.39  | 7.92   | 0.933                |
| 25.0                      | 100                                 | 6.64  | 7.92   | 0.838                |
| 25.0                      | 150                                 | 6.69  | 7.92   | 0.845                |
| 25.0                      | 200                                 | 6.86  | 7.92   | 0.866                |
| 35.0                      | 50                                  | 10.6  | 10.2   | 1.039                |
| 45.0                      | 50                                  | 13.1  | 12.7   | 1.031                |

ticles used in experiments were smaller than about 10 μm in diameter.<sup>63,64</sup> In support to the diffusion rate-determining dissolution process of vaterite was also the activation energy, calculated from the slope of the Arrhenius plot,  $\ln D_{app}$  *v.s.*  $1/T$ . The value was found to be  $E_a = 24 \pm 2$  kJ/mol and was typical of the diffusion of ions in aqueous solution.

*Kinetics of Transformation.* – All metastable modifications of calcium carbonate transform into calcite, the thermodynamically stable polymorph under the conditions of ordinary temperature and pressure at the Earth surface. The transformation of aragonite to calcite has more frequently been reported than the transformation of vaterite to calcite or to aragonite,<sup>53,65–70</sup> in spite of the assumed role that was given to vaterite in calcium carbonate natural deposits.<sup>71</sup> When the transformation of vaterite was studied, the investigation dealt either with the thermal treatment of vaterite in its dry state<sup>53,66,72,73</sup> or with the process in which vaterite seed crystals were inoculated into low supersaturated solutions.<sup>67</sup> Therefore, we decided to examine the kinetics and mechanism of vaterite transformation to calcite in a process in which vaterite was the only solid phase initially precipitated in the system and in which both vaterite and calcite formed spontaneously. The aim was also to set an adequate mathematical model of the overall process.

The kinetics of transformation was studied in aqueous solution at temperatures between 25 and 45 °C and ionic strengths between 15 and 415 mmol dm<sup>-3</sup>.<sup>12</sup> The propagation of the reaction was followed by recording pH of the solution as a function of time, and to determine the precipitate composition during the reaction we developed a fast and relatively precise procedure for quantitative analysis of vaterite-calcite mixtures, based on IR spectroscopy.<sup>74</sup> The crystal size distribution and the particle number density were determined for each experiment. No correlation was found between the temperature or the ionic strength and the number of vaterite and calcite particles formed, thus suggesting that hetero-



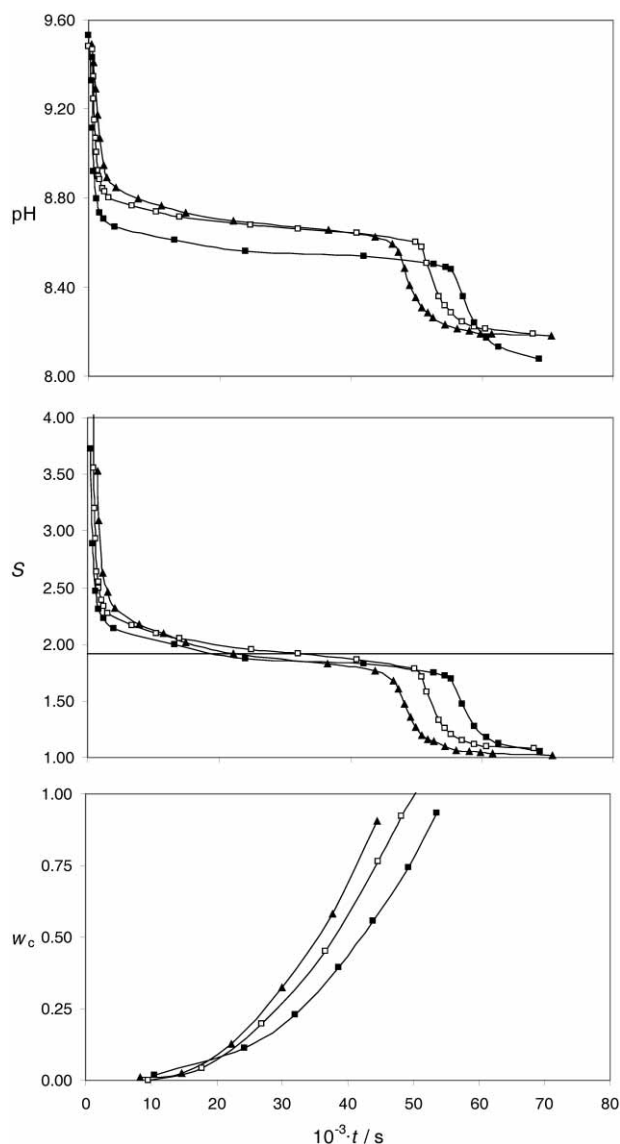


Figure 8. Changes of pH vs. time during the transformation of vaterite to calcite at 25 °C and at different initial ionic strengths: 115 (■), 215 (□) and 315 (▲) mmol dm<sup>-3</sup>. The corresponding changes of saturation ratio,  $S$ , and mass fraction of calcite in the precipitate,  $w_c$ , are shown.

geneous nucleation was responsible for the formation of both solid phases.

In the experiments in which the transformation of vaterite to calcite was studied, typical experimental step-like, pH vs. time, curves were obtained (Figure 8). The first step of the curves corresponded predominantly to the formation and growth of vaterite during which no calcite was detected in the precipitate. The second pronounced fall of pH was a consequence of the disappearance of vaterite from the system and the growth of calcite crystals becoming the only process taking place in the system. The plateau placed between the two steps reflected the simultaneous participation of three main processes: the growth and dissolution of vaterite, and the growth of

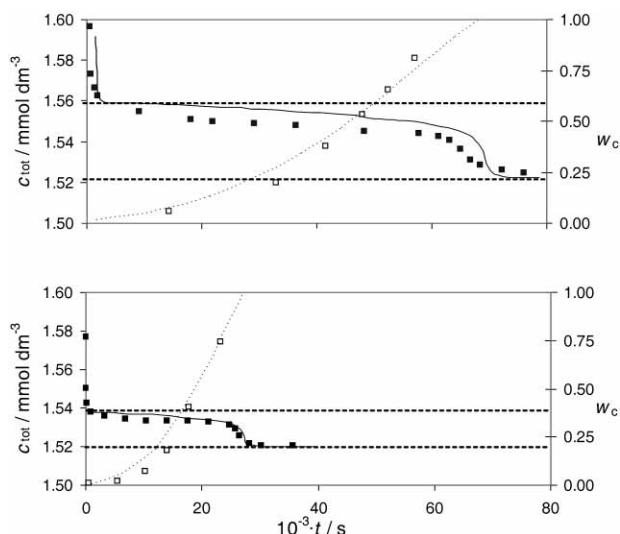


Figure 9. Plots of the total concentrations of calcium carbonate,  $c_{tot}$ , in solution and the mass fraction of calcite in the solid phase,  $w_c$ , as a function of time at different temperatures: 25 °C (above) and 45 °C (below). The corresponding model curves and the solubilities of vaterite (upper dashed lines) and calcite (lower dashed lines) are also shown.

calcite. From the pH data recorded and the known concentrations of reactants added initially to the system, the molar concentrations and the corresponding activities of all relevant species at any moment of the process were calculated. Thus, the value of the saturation ratio corresponding to vaterite being in equilibrium with the solution at 25 °C was calculated to be  $S_v/S_c = 1.92$ . Figure 9 shows the results of the experiments, performed at different temperatures. The calculated total concentration of calcium carbonate dissolved,  $c_{tot}$ , and the measured mass fraction of calcite present in the solid phase,  $w_c$ , are plotted as a function of time. The solubilities of vaterite and calcite under given conditions are indicated as upper and lower dashed lines, respectively, and the adequate curves calculated in accordance with the mathematical model are also shown. In all transformation experiments, the concentration plateaus were placed just below the solubility of vaterite. According to the kinetic model of solvent-mediated phase transformation, proposed by Davey *et al.*,<sup>75</sup> it could be concluded that the crystal growth of calcite (stable phase) was the rate determining process for the overall transformation of vaterite to calcite. This conclusion was additionally supported by a mathematical model.

The model was based on the data of mechanisms and rate constants of three main processes that influenced the rate of transformation and on the experimentally determined number densities of the crystals formed. The model also predicted changes of both the solution and the solid phase during the process. In this connection, the kinetics and mechanism of calcite crystal growth had to be determined in separate experiments.

The following differential equations for the kinetics of the processes involved were used:

(1) Crystal growth of vaterite, previously found to follow the parabolic rate law, Eq. (3),<sup>56</sup>

$$dr/dt = k_{gv} (S - 1)^2 = k_{gv} [(c - c_{sv})/c_{sv}]^2$$

(2) Dissolution of vaterite, found to be controlled by diffusion of constituent ions into solution, Eq. (5),<sup>57</sup>

(3) Crystal growth of calcite, found to be the second order surface reaction<sup>12</sup> (more about it in the section on calcite),

$$dr/dt = k_c (S - 1)^2 \quad (6)$$

where  $k_c$  is the growth rate constant of calcite.

These equations were solved numerically using the initial concentration of calcium carbonate,  $c_i = c_{tot}$ , at the time  $t = 0$ , the number of particles of both polymorphs measured in the system, and the initial radii of vaterite and calcite,  $r_v = r_c = 0$ . One of the principal assumptions of the model was that both polymorphs nucleated at the time  $t = 0$ , the growth of calcite being much slower than that of vaterite. This assumption was proved in an additional experiment.<sup>12</sup>

#### Calcite, $CaCO_3$

At ordinary temperature and pressure, calcite is a thermodynamically stable modification of calcium carbonate to which all metastable forms tend to transform. Because of its importance, mostly in sedimentary carbonate petrology but also in biology, environmental and industrial processes, this polymorph has been the subject of investigations by many authors.<sup>13–17,52,76,77</sup>

Our interest in this stable calcium carbonate modification was primarily connected with calcite being the final form of all unstable  $\rightarrow$  stable phase transitions and in this connection with its properties under different conditions.

*Seeded Crystal Growth.* – The investigation of the kinetics of this process was associated with the study of vaterite to calcite transformation.<sup>12</sup> The crystals of calcite were prepared using the method for vaterite preparation,<sup>57</sup> with a distinction that the vaterite crystals formed initially were left in the mother liquor to transform. The composition of the final product, after filtering and drying at 105.5 °C, was analysed by X-ray diffraction and IR-spectroscopy. The substance was found to be pure calcite, appearing as rhombohedral crystals with the specific surface area of 0.7 m<sup>2</sup> g<sup>-1</sup> and an average diameter of about 3 μm (Figure 10).

The growth kinetic experiments were performed under the same conditions of initial supersaturation as those of vaterite transformation, at temperatures between 10 and 55 °C and ionic strengths between 15 and 215 mmol dm<sup>-3</sup>.

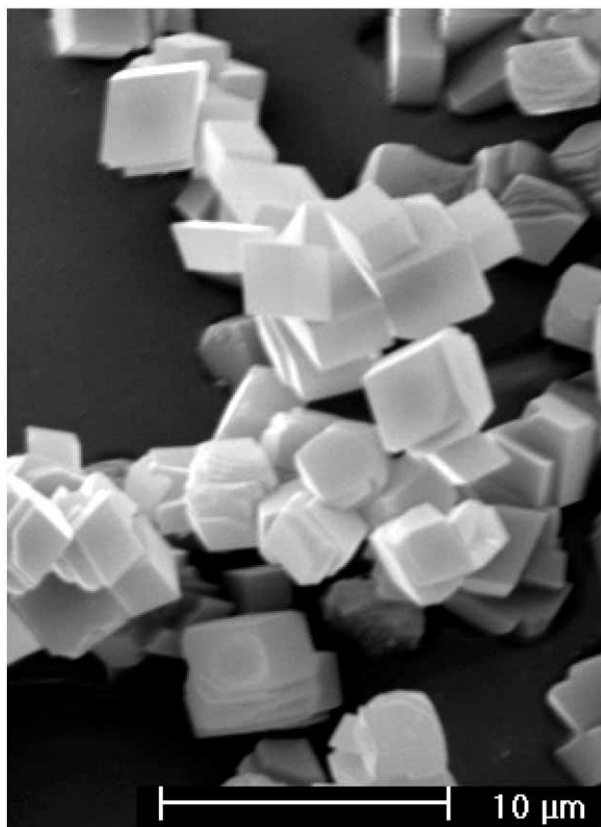


Figure 10. Scanning electron micrographs of calcite crystals.

The known amount of the calcite seeds were introduced in the system and the changes of pH were followed during the reaction. For each experiment, the composition and the particle number density of the solid phase were analysed to find out if an additional nucleation of vaterite or calcite occurred. The growth rates of calcite were calculated as described for the case of vaterite growth experiments,<sup>56</sup> using the relevant solubility product and equilibrium constants.

The plots of the square root of calcite growth rates,  $(dr/dt)^{1/2}$ , as a function of the relative supersaturation,  $S - 1$ , gave straight lines, thus indicating that the integration of ions into the spiral step or the surface diffusion was the rate determining step (see Eq. (6)).<sup>59</sup> The rate constants,  $k_c$ , found from the slopes of the straight lines at different temperatures are given in Table V. These values were used in setting the mathematical model for the transformation of vaterite to calcite,<sup>12</sup> and also for the determination of the activation energy for the crystal growth of calcite,  $E_a$ . By using the Arrhenius plot,  $\ln k$  vs.  $1/T$ , the best fitted straight line to the points was represented by

$$\ln (k_c/m \text{ s}^{-1}) = -2.446 - 6650 (T/K)^{-1} \quad (7)$$

from the slope of which the activation energy was found to be  $E_a = 55 \pm 7 \text{ kJ mol}^{-1}$ . This relatively high value is

TABLE V. Values of the rate constants of calcite seeded growth,  $k_c$ , determined at different temperatures

| $\theta / ^\circ\text{C}$ | $k_c / \text{nm s}^{-1}$ |
|---------------------------|--------------------------|
| 10.2                      | 0.006                    |
| 25.0                      | 0.014                    |
| 34.8                      | 0.049                    |
| 54.5                      | 0.122                    |

in support to the surface controlled process (most probably the integration of ions) of the calcite growth and can be placed among the values reported in the literature (from 39 to 155 kJ mol<sup>-1</sup>).<sup>67,78-81</sup>

**Dissolution.** – Generally, the dissolution process takes place in several steps following one another. When it is a question of calcite, these steps might be detachment of the constituent ions from the crystal lattice, their hydration and diffusion away from the crystal surface into the bulk solution. The rate-determining step of the overall dissolution process is the slowest among these consecutive steps. Because of the fact that almost all these steps occur with a considerable change in the heat content, a calorimetric method was applied in the study of the calcite dissolution kinetics in aqueous solutions.<sup>82</sup> The method was tested by using aqueous EDTA solutions, the medium chosen because the dissolution process was slow enough to enable the application of the calorimetry technique. Since the complexing agent was present in the system, attention was also given to the formation of the Ca-EDTA complex and its transport from the crystal surface into the bulk solution. The kinetic model describing the dissolution process and giving an estimate of the mechanism governing the process was introduced in the form of Eq. (8)

$$-dn/dt = k A_t [\text{EDTA}] / \text{mol dm}^{-3})^b \quad (8)$$

where  $n$  is the amount of solid CaCO<sub>3</sub>,  $t$  is the time,  $A_t$  is the total surface area of solid calcite at time  $t$ ,  $k$  is the rate constant of dissolution, while  $[\text{EDTA}]$  and  $b$  denote the EDTA concentration in the bulk of solution and the exponent depending on the mechanism of interaction, respectively.

Assuming that number of dissolving particles is constant and that the particles are approximately spherical, the following expression for total surface area was obtained

$$A_t = 3m_o / \rho r_o \{1 - [(n_o - n_t) / n_o]\}^{2/3} \quad (9)$$

where  $r_o$  is the initial radius of particles,  $m_o$  is the initial mass of the solid calcite of density  $\rho$ ,  $n_o$  is the initial amount of the solid CaCO<sub>3</sub> and  $n_t$  is the amount of the solid CaCO<sub>3</sub> at time  $t$ .

According to Eqs. (8) and (9), the following expression was obtained

$$\lg(-dn/dt) = \lg k_{\text{rel}} + 2/3 \lg \{1 - [(n_o - n_t) / n_o]\} \quad (10)$$

where the relative rate constant  $k_{\text{rel}}$  is defined as

$$\lg k_{\text{rel}} = \lg k + b \lg [\text{EDTA}] / \text{mol dm}^{-3} + \lg (3 m_o / \rho r_o) \quad (11)$$

Enthalpy is proportional to the extent of the reaction, so that the change of enthalpy could be used for evaluation of the reaction rate. It is obvious that this method could be applied only for slow reactions. The following relationship was used

$$-dn/dt = (C/\Delta_r H) (dT/dt) \quad (12)$$

where  $T$  is the temperature,  $C$  is the heat capacity of the system and  $\Delta_r H$  is the overall reaction enthalpy.

The calcium carbonate used in the experiments (Riedel, Germany) was found to be calcite (shown by X-ray diffraction) with the specific surface area of 0.51 m<sup>2</sup> g<sup>-1</sup>, which corresponds to the average particle diameter of an equivalent sphere of  $\approx 3 \mu\text{m}$ . The calorimeter used was an isoperibolic reaction type,<sup>83</sup> and the temperature was kept at 25.0 °C, changing during the experiment less than 0.005 °C.

The thermograms obtained were interpreted by considering the heat evaluation due to the dissolution reaction and the heat transfer in the calorimeter. The interpretation of the reaction kinetics was based on the change of the particle surface area during dissolution. It was found that the dissolution process was the first-order reaction with respect to the surface area, indicating that the detachment of the Ca-EDTA complex from the solid phase surface was the controlling mechanism. The first-order reaction was reported previously for calcite.<sup>84,85</sup> The relative rate constant was determined to be  $\lg(k_{\text{rel}}/\text{mol s}^{-1}) = -4.71 \pm 0.01$  and the enthalpy of calcite dissolution  $\Delta_d H = -12 \text{ kJ mol}^{-1}$ . All this confirms the applicability of the proposed method to other systems and the possibility of using it in the study of precipitation kinetics.

**Technological Application.** - Apart from their inherent aptness for the pure academic studies, calcium carbonates are an important technological product, produced on large scale (so-called precipitated calcium carbonate, PCC). PCC has a wide application as filler in paper, plastic, paint and pharmaceutical products, and owing to such a variety of applications needs to have different physical and chemical properties. Among these properties, particle size, specific surface area and morphology are the most important. Therefore, the precipitation conditions similar to those found in the large-scale production of calcium car-

bonates, particularly calcite, were studied in this laboratory.

The large scale of PCC production is most often performed by a process of slaked lime carbonation, *i.e.* by bubbling  $\text{CO}_2$  gas through an aqueous  $\text{Ca}(\text{OH})_2$  suspension in a batch reactor. We investigated a semicontinuous production of PCC by slaked lime carbonation, in a custom built bench-scale chemical reactor, controlled by means of the electronics and software for the personal computer.<sup>86</sup> Such a hardware enabled us to systematically vary a range of experimental parameters (temperature, supersaturation, gas mixture flow rate, stirring rate and mass concentration of  $\text{Ca}(\text{OH})_2$  suspension) in order to produce calcite crystals, with different morphological characteristics (rhombohedral, truncated prismatic, scalenohedral, spheroidal or chain-like agglomerates) or with a specific surface area. Moreover, in order to identify the effects of the experimental parameters on the particular PCC and the process properties (morphology, specific surface area,  $\text{CO}_2$  conversion), an empirical approach based on the experimental design techniques was employed. On the basis of the performed experiments and analysis, it was found that temperature and conductivity significantly influenced the PCC morphology: at low temperatures and high conductivities, submicrometric calcite crystals with a large specific surface area were produced, whereas at high temperatures and low conductivities well-crystallized micrometric calcite of low specific surface area precipitated. It was also found that the  $\text{CO}_2$  conversion rate was significantly influenced by the stirring rate, conductivity and the gas mixture flow rate.

#### *Influence of Foreign Ions and Molecules*

The formation of a particular solid phase, its morphological properties and crystal habit depend on precipitation conditions, such as the initial supersaturation, temperature, pH, mixing and stirring conditions and the presence of impurities and additives.<sup>39,55,56,87</sup> Consequently, most of these factors can govern the rate and the mechanisms of the precipitation processes, among which additives and impurities of either inorganic or organic nature play an important role. In recent years, the most intensively investigated additives concerning precipitation of calcium carbonates were soluble polymeric and special functional low molecular weight additives,<sup>88–93</sup> as well as the protein macromolecules isolated from some living organisms in which  $\text{CaCO}_3$  was found to be a biomineral component.<sup>94–97</sup> Among the inorganic ions, the influence of metal ions, divalent metal ions in particular, are of special importance, because these ions may co-precipitate with calcium carbonates, either being adsorbed on the particle surface or forming solid solutions and occlusions.<sup>98,99</sup> The mode of their incorporation is not always easy to define. In order to study the effect of foreign ions on the formation and structure of calcium carbonate

polymorphs, their mode and sites of incorporation in the crystal lattice and their influence on the morphology, we used a number of analytical methods and techniques.

*Effect of Divalent Cations.* – Among the possible divalent cations, the ones essential for living organisms and/or substitutive for  $\text{Ca}^{2+}$  ( $\text{Mg}^{2+}$ ,  $\text{Mn}^{2+}$ ,  $\text{Cu}^{2+}$ ,  $\text{Sr}^{2+}$ ,  $\text{Cd}^{2+}$ ,  $\text{Ba}^{2+}$  and  $\text{Pb}^{2+}$ ) were used to study the interactions with vaterite and calcite.<sup>100</sup> For this purpose, atomic absorption spectroscopy (AAS), optical and scanning electron microscopy (SEM), X-ray diffraction (XRD) and electron paramagnetic (EPR) spectroscopy, along with other standard analytical techniques were used. Vaterite and calcite crystals were prepared by spontaneous precipitation under defined conditions.<sup>56,57</sup> XRD analyses showed rather broad diffraction lines for vaterite and much sharper for calcite (Figure 11). Calcite crystallized in well-defined rhombohedra, whereas vaterite spherical particles, as estimated from the observed broadening, were aggregates of crystallites of 25–35 nm. Doping with foreign cations was performed by adding particular cation(s) in the calcium reactant component.

The fractions of metal ions incorporated into the solid phase were determined by AAS. All cations, except  $\text{Cu}^{2+}$ , were found to be incorporated in vaterite and the

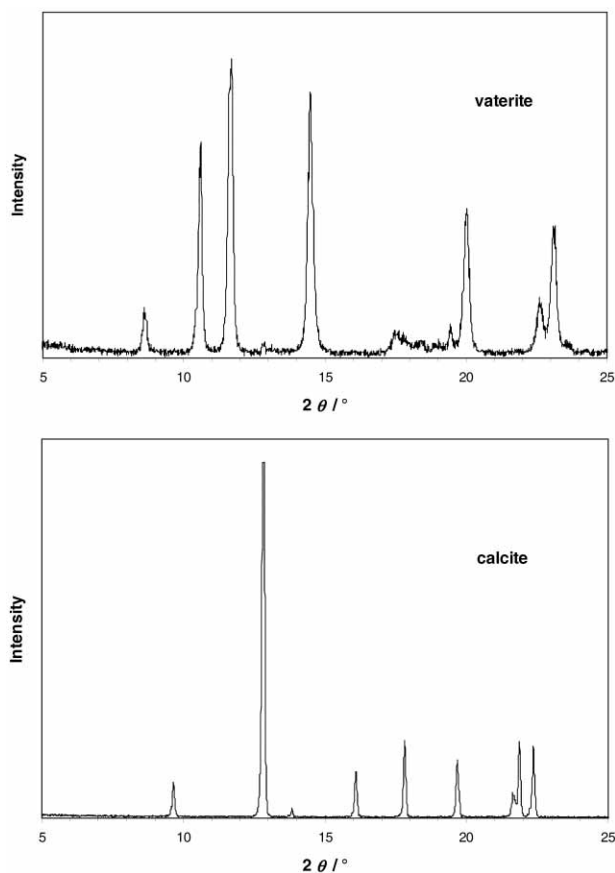


Figure 11. Characteristic parts of XRD patterns of vaterite and calcite.



uptake of  $\text{Mn}^{2+}$  was about the same no matter whether an additional cation was also incorporated or not. The presence of  $\text{Mn}^{2+}$  stimulated the incorporation of  $\text{Pb}^{2+}$  and  $\text{Mg}^{2+}$ , and the amount of  $\text{Mg}^{2+}$  in the solid phase increased with the increase of  $\text{Mg}^{2+}$  concentration in the system. The uptake of  $\text{Mn}^{2+}$ ,  $\text{Cd}^{2+}$  and  $\text{Pb}^{2+}$  by vaterite was much larger than by calcite.

$\text{Ba}^{2+}$  (ionic radius = 1.35 Å) and  $\text{Mg}^{2+}$  (ionic radius = 0.72 Å) ions substituting for  $\text{Ca}^{2+}$  (ionic radius = 0.99 Å) in the vaterite crystal lattice increased the average vaterite particle diameter from *ca.* 3 µm of the pure vaterite spheres to *ca.* 4.5 µm and *ca.* 5.3 µm in the case of  $\text{Mg}^{2+}$  and  $\text{Ba}^{2+}$  incorporation, respectively. Doping with  $\text{Ba}^{2+}$  also caused an asymmetric change in the crystal lattice of vaterite. Most probably solid solutions were formed.<sup>101–103</sup> On the other hand,  $\text{Mg}^{2+}$  did not cause detectable distortion of the vaterite lattice, probably because being smaller than  $\text{Ca}^{2+}$  and was incorporated in interstitial positions of the vaterite crystal. However,  $\text{Mg}^{2+}$  affected the shape of vaterite particles, changing it to a disc-like.

In order to study the local environment in vaterite and calcite crystal lattice by EPR spectroscopy,  $\text{Mn}^{2+}$  was used as a paramagnetic substitute for  $\text{Ca}^{2+}$ . Previously, EPR spectra of  $\text{Mn}^{2+}$  impurities in calcite were reported by many authors,<sup>104–106</sup> but there were no literature data regarding the EPR spectrum of  $\text{Mn}^{2+}$  in vaterite. We found that  $\text{Mn}^{2+}$  ions were incorporated into vaterite in at least two different environments: (a) segregated into clusters, probably in the growth zones and (b) substituted for  $\text{Ca}^{2+}$  in the vaterite lattice. The environment of  $\text{Mn}^{2+}$  substituted for  $\text{Ca}^{2+}$  in the vaterite lattice was of lower symmetry than in the calcite lattice.

The EPR spectra of  $\text{Mn}^{2+}$  revealed the formation of calcite due to the presence of  $\text{Cd}^{2+}$  or  $\text{Pb}^{2+}$  in the vaterite-precipitating system. The presence of  $\text{Cd}^{2+}$  and  $\text{Pb}^{2+}$  in the calcites also caused a perturbation of the crystal lattice, which was reflected in the local environment of  $\text{Mn}^{2+}$ . These results were confirmed by EPR spectra of the free radicals formed by  $\gamma$ -irradiation of vaterite and calcite in the absence of  $\text{Mn}^{2+}$ . In elucidation of the calcite formation in the vaterite phase we also used the valence electron configurations of  $\text{Cd}^{2+}$  and  $\text{Pb}^{2+}$ , which, in our opinion, has an important role in the interaction of foreign cations with carbonates.<sup>107</sup> The configurations of  $\text{Cd}^{2+}$  and  $\text{Pb}^{2+}$  were determined by d and f electrons, which can participate in the donor-acceptor bond formation. Since the crystal field around these cations is thus of different symmetry, the formation of the calcite structure in the vaterite system is favoured.

A number of free radicals were identified by studying EPR spectra of pure vaterite, such as  $\cdot\text{CO}_3^-$  holes freely rotating at the surface of crystals,  $\cdot\text{CO}_2^-$  frozen in the matrix and  $\cdot\text{CO}_2^-$  freely rotating. The alkaline-earth metal cations ( $\text{Mg}^{2+}$ ,  $\text{Sr}^{2+}$  and  $\text{Ba}^{2+}$ ) were found not to affect the formation and stability of these free radicals

and with their closed electron valence shells most probably substitute for  $\text{Ca}^{2+}$  not perturbing greatly the vaterite crystal lattice.  $\text{Cu}^{2+}$  and  $\text{Cd}^{2+}$  were found to trap electrons by forming  $\text{Cu}^+$  and  $\text{Cd}^+$ , which led to an increased formation of freely rotating  $\cdot\text{CO}_3^-$  holes in the near neighbourhood. With their 3d and 4d, electron valence shell configurations do not incorporate easily into the vaterite structure and are located mostly at its surface. Only small amounts of these cations incorporate in the vaterite lattice and perturb it by inducing different crystal field symmetry. As a consequence, this may lead to the formation of calcite in the vaterite phase. Our further EPR studies of  $\text{Cd}^{2+}$  incorporation in vaterite showed the existence of two paramagnetic centres induced by cadmium doped to vaterite which were most probably due to  $\text{Cd} \leftarrow \text{O}^-$ .<sup>108</sup> The motion of one of these centres was completely frozen, which assumed that the centre was probably incorporated between the tightly packed crystallites inside the vaterite spherical particles or even inside the crystallites. The other centre also originated from an electron trapped on oxygen but most likely located on the surface of vaterite spherulites. On the basis of the location of these paramagnetic centres in vaterite, the sites of  $\text{Cd}^{2+}$  incorporation were determined.

*Effect of Inorganic Anions.* – Besides the investigations represented above, a systematic study of the influence of foreign ions was undertaken, primarily the influence of  $\text{Mg}^{2+}$  in conjunction with some common anions, such as  $\text{SO}_4^{2-}$ ,  $\text{NO}_3^-$  and  $\text{Cl}^-$ , on the morphology, crystal size distribution, composition, structure and specific surface area of the precipitated crystals. It has been shown that the polymorphism, morphology and structural properties of calcium carbonate can be controlled by the use of specific additives, macromolecules, small organic molecules and inorganic ions.<sup>109–116</sup> Among the inorganic components,  $\text{Mg}^{2+}$  has a particularly important role. Under certain conditions, it can act either as a very effective inhibitor of nucleation and/or crystal growth of calcite<sup>110,112</sup> or as a promoter of aragonite nucleation.<sup>117</sup> The aim of our studies was principally to investigate the effects of both the cation and the anions on the physical-chemical properties of the precipitated calcium carbonate.<sup>118</sup>

Calcium carbonate was precipitated by mixing calcium hydroxide and carbonic acid solutions, the latter solution being prepared by bubbling a high-grade carbon dioxide stream into water until saturation was achieved. In order to study the effect of different anions on the precipitate properties, the respective salt ( $\text{MgSO}_4$ ,  $\text{Mg}(\text{NO}_3)_2$ ,  $\text{MgCl}_2$ ,  $\text{Na}_2\text{SO}_4$ ,  $\text{NaNO}_3$  or  $\text{NaCl}$ ) was added to the calcium hydroxide solution. The experiments were conducted at 25 °C and the propagation of the reaction was followed by measuring the pH of the solution. The results of the investigations showed that the incorporation of magnesium into the calcite crystal lattice depended on the nature of the co-anions present in the system. For the

molar ratios  $c_i(\text{Mg}^{2+})/c_i(\text{Ca}^{2+}) = 1:1$  and  $2:1$  of the initial solution concentrations, the magnesium content in calcite crystals decreased in the series  $\text{MgSO}_4 > \text{Mg}(\text{NO}_3)_2 > \text{MgCl}_2$ . The highest magnesium content in the calcite lattice was achieved in the systems with no additional anions (except  $\text{OH}^-$ ), *i.e.* in the systems in which the dissolved magnesium hydroxide was used as the source of magnesium. It was also shown that there was a clear relation between the morphological properties of calcites containing magnesium and the concentration of the corresponding anion, as well as the amount of magnesium incorporated into the calcite lattice. The addition of sulphate ions, alone, caused the formation of spherical aggregates of the originally rhombohedral calcite crystals. Calcite was chosen because of its thermodynamic stability under standard conditions and also because of the existence of extensive data on calcite in the literature. EPR measurements of magnesium calcites precipitated from solutions of different anions revealed different modes and extents of magnesium incorporation.

In order to investigate the role of anions separately from foreign cations, the precipitation system was prepared in the same way as described above, *i.e.* calcite was precipitated by using calcium hydroxide and carbonic acid solutions as reactants. Thus, any possible effect of ions other than the constituent ions or products of autoprotolysis of water ( $\text{Ca}^{2+}$ ,  $\text{CO}_3^{2-}$ ,  $\text{HCO}_3^-$ ,  $\text{H}_3\text{O}^+$ ,  $\text{OH}^-$ ) on the precipitation of calcite was avoided. Calcite prepared in such a way can be used as a reference for a number of different studies. Foreign anions were added to the system in the form of calcium salts ( $\text{CaSO}_4$ ,  $\text{Ca}(\text{NO}_3)_2$  and  $\text{CaCl}_2$ ). A relatively narrow range of the co-anion total initial concentrations,  $c_i(\text{anion}) = 1.0 \times 10^{-4}$  to  $1.0 \times 10^{-3}$  mol dm<sup>-3</sup>, was investigated at a moderate relative initial supersaturation,<sup>12,118</sup>  $S - 1 = 10.38$ , and at 25 °C.<sup>119</sup> This was necessary in order to minimise the influence of the kinetic factors, since changes in nucleation and/or growth rates can cause changes in the growth mechanisms and, consequently, influence the co-anion incorporation. The aim was to shed more light upon the mode and sites of incorporation of these anions into the calcite lattice. For this purpose, a combination of SEM, XRD, FT-IR, differential thermal analysis (DTA), ion chromatography (IC) and EPR spectroscopy was used. The local environment by EPR spectroscopy was studied by using  $\text{Mn}^{2+}$  as a paramagnetic substitute for  $\text{Ca}^{2+}$ .

Under the given experimental conditions, calcite crystals were formed by heterogeneous nucleation and were considerably monodispersed and small in size, exhibiting a distribution maximum at about 7 µm. The crystals were rhombohedral and rather uniformly shaped, regardless of the co-anions being added to the precipitation system or not. Only at the highest concentrations of sulphate ions used in the experiments ( $c_i(\text{anion}) = 1.0 \times 10^{-3}$  mol dm<sup>-3</sup>), a slight tendency toward crystal aggregation was obtained. As observed earlier,<sup>118</sup> the effect of sulphate ions

on the aggregation of calcite crystals was more pronounced in the systems in which the initial supersaturation, and consequently the growth rate, was much higher ( $S - 1 > 30$ ,  $\text{pH}_i > 10.5$ ). In that case, the spherical aggregates of calcite crystals were obtained.

EPR spectra showed that the distortion of the calcite lattice from axial symmetry was achieved by the addition of  $\text{SO}_4^{2-}$  or  $\text{Cl}^-$ , but no effect of the kind was obtained when  $\text{NO}_3^-$  was added. The addition of  $\text{SO}_4^{2-}$  also showed a pronounced uniaxial strain of the threefold axis. This suggested that although  $\text{SO}_4^{2-}$  ions match the charge of the calcite  $\text{CO}_3^{2-}$  groups, they produce larger uniaxial strain than  $\text{NO}_3^-$  or  $\text{Cl}^-$ . Similar results were obtained by XRD. It was shown that  $\text{NO}_3^-$  did not have any effect on the diffraction pattern of calcite and such was the effect of chloride ions. However, chloride ions caused a slight increase of the diffraction peak full width half maxima (FWHM) as the initial concentration of these anions increased in the system. Since this effect indicated a reduction of the overall crystallinity, this suggested a probable incorporation of chloride ions into the calcite crystal structure. Sulphate ions, expectedly, showed the pronounced effect because they were not only incorporated in the calcite structure but they also induced a reduction of calcite crystallinity.

According to the undertaken analyses of calcite samples, the respective co-anions were incorporated into the calcite crystal lattice to a certain extent. The incorporation of sulphate ions was found to be the most extensive. Therefore, further discussion on the co-anion incorporation will be reduced to the effect of the sulphate ion. Thus, the DTA results of pure and sulphate doped calcites supported the conclusion of sulphate being incorporated into the calcite structure. An endothermic peak at 810 °C obtained for pure calcite, denoting its decomposition by loss of  $\text{CO}_2$ , was shifted by 15 °C toward lower temperatures when the sample was prepared by the addition of sulphate ions. Such a shift could be induced only by the sulphate ions incorporated into the calcite structure, thus causing its destabilisation. IC also showed that the content of sulphate ions in calcite increased by increasing the amount of  $\text{CaSO}_4$  added to the precipitation system.

Based on the XRD, EPR spectroscopy and IC analyses, a simplified model which attempts to explain the mode and sites of sulphate ion incorporation into the calcite crystal lattice was proposed. According to the model, carbonate ions are partially substituted by sulphate ions causing a distortion of the calcite unit cell. The degree of disorder along the *c* axis is much higher than along the other two axes, which is a consequence of substitution of the tetrahedral sulphate for the planar carbonate ions (Figure 12).

*Influence of Organic Substances.* – The precipitation of calcium carbonate in natural waters, especially in seawater, is often influenced by the presence of dissolved substan-

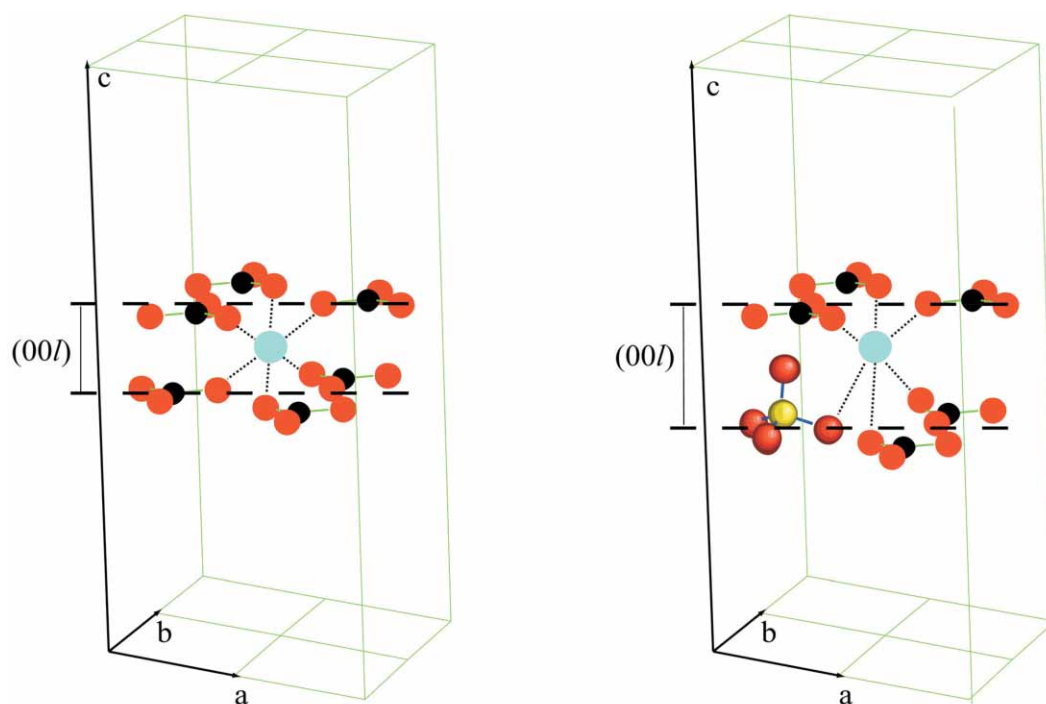


Figure 12. Schematic representation of the model showing: (a) the calcite crystal lattice cell, and (b) the possible mode and site of sulphate ion incorporation (with permission of the European Journal of Inorganic Chemistry).

ces, such as  $Mg^{2+}$ , phosphates and organic substances. Most of these substances act as inhibitors of calcium carbonate precipitation,<sup>120–122</sup> yet if the precipitation occurs, these substances often act as promoters of a certain calcium carbonate polymorph, aragonite in particular.<sup>123</sup> The aim of the study presented in this section was to give an insight into the influence of organic matter on the precipitation of calcium carbonates and on the surface charge of the particles formed. The precipitation was brought about with solutions containing calcium and carbonate components in the concentrations similar to those in seawater. The ionic strength was adjusted by the addition of NaCl into the calcium reactant solution, and the organic substance (propionic, citric or fulvic acid) was added into the carbonate reactant solution. The precipitation process was followed by recording pH, the electrophoretic mobilities of the resulting solid particles were measured and the electrokinetic potentials,  $\zeta$ , calculated. The particles obtained were found to be vaterite of the average size of  $3.0\ \mu\text{m}$ . Their number was of the order of  $10^7$  per  $\text{cm}^3$  and the specific surface area was  $9.0\ \text{m}^2\ \text{g}^{-1}$ . The electrophoretic mobility measured when the system was assumed to be in equilibrium showed a positively charged surface,  $\zeta = 18.1\ \text{mV}$ , at  $\text{pH} = 8.3$ . By changing pH of the system, the  $\zeta$ -potential of vaterite was found to be positive in the range from  $\text{pH} = 7.5$  to  $10.0$ , the isoelectric point being  $\text{pH}_{\text{iep}} = 9.9$ . It was also found that the absolute value of the  $\zeta$ -potential of calcium carbonate depended largely on the solid phase amount and the surface area of the sample.

Fulvic acid was found to be the inhibitor of both the nucleation and crystal growth of calcium carbonate. The addition of even very low concentrations of fulvic acid to vaterite significantly reduced the  $\zeta$ -potential and reversed it to negative. This was a clear indication that fulvic acid adsorbed on the positively charged sites of vaterite surface, thus disabled its crystal growth. Because of such findings, it is not probable to observe the precipitation of calcium carbonate in natural seawater, where fulvic acid is a common substance, or to find positively charged calcium carbonate particles.

Citric acid reduced the positive charge of vaterite particles causing a partial inhibition of the vaterite crystal growth. By increasing its concentration in the system, citrate completely inhibited the precipitation of vaterite, by adsorbing on the growth sites at the vaterite surface, and promoted the formation of calcite.

Propionic acid showed no such effects on the precipitation and surface charge of the vaterite particles formed. This was an indication that probably simple organic molecules would not influence the calcium carbonate precipitation and their charge in natural waters.

## CONCLUSIONS

Extensive and systematic investigations of calcium carbonate polymorphs and hydrates have been performed in the Laboratory for Precipitation Processes during the last nearly twenty years. The concentration domains for the formation of initial pure modifications, subsequently

used in the investigations, have been determined. Besides, the thermodynamic parameters, such as the temperature dependence of the solubility products of amorphous calcium carbonate, calcium carbonate monohydrate and hexahydrate, have also been determined:

amorphous  $\text{CaCO}_3$

$$-\log(K_s^\circ) = 6.1987 + 0.005336 (\theta/^\circ\text{C}) + 0.0001096 (\theta/^\circ\text{C})^2$$

$\text{CaCO}_3 \cdot \text{H}_2\text{O}$

$$-\log(K_s^\circ) = (7.050 \pm 0.029) + (0.000159 \pm 0.00019) (\theta/^\circ\text{C})^2$$

$\text{CaCO}_3 \cdot 6\text{H}_2\text{O}$

$$-\log(K_s^\circ) = 7.1199 + 0.011756 (\theta/^\circ\text{C}) + 0.000075556 (\theta/^\circ\text{C})^2$$

The prepared solid phases have been thoroughly characterized by means of different instrumental techniques, such as electron microscopy, IR and/or EPR spectroscopy, and some of the results obtained are the first of the kind described in the scientific literature. This also relates to the results obtained in the study of the influence of inorganic and organic additives on the vaterite and calcite formation, and to the incorporation of these additives into their crystal lattices.

On the basis of the data on the crystal growth and dissolution kinetics of different calcium carbonate phases, it may be concluded that for a given range of conditions, the vaterite and calcite growth, as well as the calcite dissolution, are predominantly surface controlled processes. However, the dissolution of vaterite and calcium carbonate monohydrate is controlled by diffusion of ions away from the particles' surface to the bulk of solution.

The precipitation of calcium carbonates has also been investigated in the systems in which precipitation was initiated by carbonation of  $\text{Ca}(\text{OH})_2$  suspension, which is a common way of the large-scale calcium carbonate production. The experiments and statistical analysis have revealed that submicrometric calcite crystals with a high specific surface area can be produced at low temperatures and high conductivities, whereas micrometric calcite can be produced at relatively high temperatures and low conductivities.

*Acknowledgement.* - The financial support from the Ministry of Science, Education and Sports of the Republic of Croatia (project No. 098-0982904-2951) is gratefully acknowledged.

## REFERENCES

- O. Söhnel and J. Garside, *Precipitation: Basic Principles and Industrial Applications*, Butterworth-Heinemann Ltd., London, 1992.
- A. E. Nielsen, *Croat. Chem. Acta* **42** (1970) 319–333 (and the references therein).
- Lj. Brečević and D. Kralj, *Kinetics and Mechanisms of Crystal Growth in Aqueous Systems*, in: N. Kallay (Ed.), *Interfacial Dynamics*, Surfactant Sciens Series, Vol. 88, Marcel Dekker, Inc., New York, 2000, pp. 435–474.
- W. Ostwald, *Lehrbuch für allgemeine Chemie*, Vol II, Engelmann, Leipzig, 1902.
- Lj. Brečević and H. Füredi-Milhofer, *The Transformation of Amorphous Calcium Phosphate into Crystalline Hydroxyapatite*, in: J. W. Mullin (Ed.), *Industrial Crystallization*, Plenum Press, New York, 1976, pp. 277–283.
- C. H. Bamford and C. F. H. Tipper, *Comprehensive Chemical Kinetics*, Vol. 22, *Reactions in the Solid State*, Elsevier, Amsterdam, 1980.
- P. T. Cardew, R. J. Davey, and A. J. Ruddick, *J. Chem. Soc., Faraday Trans.* **80** (1984) 659–668.
- A. L. Boskey and A. S. Posner, *J. Phys. Chem.* **77** (1973) 2313–2317.
- P. T. Cardew and R. J. Davey, *Proc. Roy. Soc. London A* **398** (1985) 415–428.
- Lj. Brečević, D. Škrtić, and J. Garside, *J. Cryst. Growth* **74** (1986) 399–408.
- R. J. Davey, A. J. Ruddick, P. D. Guy, B. Mitchell, S. J. Maginn, and L. A. Polywka, *J. Phys., D: Appl. Phys.* **24** (1991) 176–185.
- D. Kralj, Lj. Brečević, and J. Kontrec, *J. Cryst. Growth* **177** (1997) 248–257.
- S. Weiner and L. Addadi, *J. Mater. Chem.* **7** (1997) 689–702.
- D. J. Sutor and L. I. Wilkie, *Clin. Chim. Acta* **79** (1977) 119–127.
- R. V. Rege and E. W. Moore, *J. Clin. Invest.* **77** (1986) 21–26.
- R. L. Folk, *Petrology of Sedimentary Rocks*, Hemphill Publishing Company, Austin, 1980.
- F. Ramisch, M. Dittrich, C. Mattenberger, B. Wehrli, and A. Wüest, *Geochim. Cosmochim. Acta* **63** (1999) 3349–3356.
- G. Falini, *Int. J. Inorg. Mater.* **2** (2000) 455–461.
- S. Mann, *Biomaterialization: Principles and Concepts in Bioinorganic Materials Chemistry*, Oxford University Press, Oxford, 2001.
- H. Cölfen, *Curr. Opin. Colloid Interface Sci.* **8** (2003) 23–31.
- G. Dorfmüller, *Deut. Zuckerrind.* **63** (1938) 1217–1219.
- Lj. Brečević and A. E. Nielsen, *J. Cryst. Growth* **98** (1989) 504–510.
- F. A. Andersen and Lj. Brečević, *Acta Chem. Scand.* **45** (1991) 1018–1024.
- J. Pelouse, *Ann. Chim. Phys.* **48** (1831) 301–307.
- J. Pelouse, *C. R. Acad. Sci.* **60** (1860) 429–432.
- J. Johnston, H. E. Merwin, and E. D. Williamson, *Am. J. Sci.* **41** (1916) 473–512.
- J. Hume and B. Topley, *J. Chem. Soc.* (1926) 2932–2934.
- B. Dickins and W. E. Brown, *Inorg. Chem.* **9** (1970) 480–486.
- Lj. Brečević and A. E. Nielsen, *Acta Chem. Scand.* **47** (1993) 668–673.
- H. Effenberger, *Monatsh. Chem.* **112** (1981) 899–909.



31. W. Sterzel and E. Charinsky, *Spectrochim. Acta, Part A*, **24** (1968) 353–360.
32. N. L. Plummer and E. Busenberg, *Geochim. Cosmochim. Acta* **46** (1982) 1011–1040.
33. F. Krauss and W. Schriver, *Z. Anorg. Allgem. Chem.* **188** (1930) 259–273.
34. D. G. Sapozhnikov and A. I. Tsvetkov, *Dokl. Akad. Nauk SSSR* **124** (1959) 131–133.
35. G. F. Taylor, *Am. Mineral.* **60** (1975) 690–697.
36. P. L. Broughton, *Contrib. Mineral. Petrol.* **36** (1972) 171–174.
37. D. J. J. Kinsman and H. D. Holland, *Geochim. Cosmochim. Acta* **33** (1969) 1–17.
38. Ph. G. Malone and K. M. Towe, *Marine Geol.* **9** (1970) 301–309.
39. R. Brooks, L. M. Clark, and E. F. Thurston, *Phil. Trans. Roy. Soc., Ser. A*, **243** (1950) 145–167.
40. H. Hull and A. G. Turnbull, *Geochim. Cosmochim. Acta* **37** (1973) 685–694.
41. F. Lipman, *Naturwiss.* **46** (1959) 553–554.
42. I. Kohatsu and J. W. McCauley, *Am. Mineral.* **58** (1973) 1102.
43. R. Debuyst, F. Dejehet, and S. Idrissi, *Radiat. Prot. Dosim.* **47** (1993) 659–664.
44. D. Kralj and Lj. Brečević, *Colloids Surf., A* **96** (1995) 287–293.
45. I. W. Duedall and D. E. Buckley, *Nature (London) Phys. Sci.* **234** (1971) 39–40.
46. Powder Diffraction File, Inorganic Vol., Table No. 29–306, International Centre for Diffraction Data, Swarthmore, PA, 1987.
47. D. L. G. Rowlands and R. K. Webster, *Nature Phys. Sci.* **229** (1971) 158.
48. J. D. C. McConnell, *Mineral. Mag.* **32** (1960) 535–545.
49. D. J. Sutor and S. E. Wooley, *Science* **159** (1968) 1113–1114.
50. A. Hall and J. D. Taylor, *Mineral. Mag.* **38** (1971) 521–522.
51. E. Dalas and P. G. Koutsoukos, *Geothermics* **18** (1989) 83–88.
52. K. Rankama and T. G. Sahama, *Geochemistry*, University Chicago Press, 1950, p. 215.
53. A. G. Turnbull, *Geochim. Cosmochim. Acta* **37** (1973) 1593–1601.
54. O. Söhnle and J. W. Mullin, *J. Cryst. Growth* **60** (1982) 239–250.
55. A. G. Xyla and P. G. Koutsoukos, *J. Chem. Soc., Faraday Trans. I*, **85** (1989) 3165–3172.
56. D. Kralj, Lj. Brečević, and A. E. Nielsen, *J. Cryst. Growth* **104** (1990) 793–800.
57. D. Kralj, Lj. Brečević, and A. E. Nielsen, *J. Cryst. Growth* **143** (1994) 269–276.
58. A. E. Nielsen and O. Söhnle, *J. Cryst. Growth* **11** (1971) 233–242.
59. A. E. Nielsen, *J. Cryst. Growth* **67** (1984) 289–310.
60. C. W. Davies, *Ion Association*, Butterworths, London, 1962, p. 41.
61. R. A. Robinson and R. H. Stokes, *Electrolyte Solutions*, 2nd ed., Butterworths, London, 1959, p. 468.
62. A. E. Nielsen, *Croat. Chem. Acta* **60** (1987) 531–539.
63. A. E. Nielsen, *Croat. Chem. Acta* **53** (1980) 255–279.
64. A. E. Nielsen, *Precipitates: Formation, Coprecipitation and Aging*, in: I. M. Kolthoff and P. J. Elving (Eds.), *Treatise on Analytical Chemistry*, 2nd ed., Wiley, New York, 1983, pp. 269–347.
65. J. L. Bischoff, *Am. Mineral.* **54** (1969) 149–155.
66. B. Fubini and F. S. Stone, *J. Mater. Sci.* **16** (1981) 2439–2448.
67. T. Ogino, T. Suzuki, and K. Sawada, *J. Cryst. Growth* **100** (1990) 159–167.
68. K. Sawada, T. Ogino, and T. Suzuki, *J. Cryst. Growth* **106** (1990) 393–399.
69. C. Tartis, P. Leroy, R. Letolle, and P. Blanc, *CR Acad. Sci. Paris* **311** (1990) 1297–1301.
70. D. Chakraborty, V. K. Agarwal, S. K. Bhatia, and J. Bel-lare, *Ind. Eng. Chem. Res.* **33** (1994) 2187–2197.
71. K. Rankama and T. G. Sahama, *Geochemistry*, University Chicago Press, Chicago, 1950, p. 215.
72. M. Maciejewski, H. R. Oswald, and A. Reller, *Thermo-chim. Acta* **234** (1994) 315–328.
73. J. Perić, M. Vučak, R. Krstulović, Lj. Brečević, and D. Kralj, *Thermochim. Acta* **277** (1996) 175–186.
74. F. A. Andersen and D. Kralj, *Appl. Spectroscopy* **45** (1991) 1748–1751.
75. R. J. Davey, P. T. Cardew, D. McEwan, and D. E. Sadler, *J. Cryst. Growth* **79** (1986) 648–653.
76. R. M. Garrels and F. T. Mackenzie, *Evolution of Sedimen-tary Rocks*, Norton, New York, 1971, p. 397.
77. J. M. Zachara, C. E. Cowan, and C. T. Resch, *Geochim. Cosmochim. Acta* **55** (1991) 1549–1562.
78. H. N. S. Wiechers, P. Sturrock, and G. v. R. Marais, *Water Res.* **9** (1975) 835–845.
79. T. F. Kazmierczak, M. B. Tomson, and G. H. Nancollas, *J. Phys. Chem.* **86** (1982) 103–107.
80. P. G. Koutsoukos and C. G. Kontoyanniss, *J. Chem. Soc., Faraday Trans. I* **80** (1984) 1181–1192.
81. S. Takasaki, K. I. Parsieglä, and J. L. Katz, *J. Cryst. Growth* **143** (1994) 261–268.
82. N. Kallay, V. Tomašić, S. Žalac, and Lj. Brečević, *J. Col-loid Interface Sci.* **188** (1997) 68–74.
83. Vl. Simeon, *Arh. Hig. Rada* **24** (1973) 233–259.
84. R. G. Compton, K. L. Pritchard, and P. R. Unwin, *J. Chem. Soc., Faraday Trans. I* **85** (1989) 4335–4366.
85. Ch. A. Brown, R. G. Compton, and Ch. A. Narramore, *J. Colloid Interface Sci.* **160** (1993) 372–379.
86. M. Ukrainczyk, J. Kontrec, V. Babić-Ivančić, Lj. Brečević and D. Kralj, *Powder Technol.* **171** (2007) 192–199.
87. J. R. Clarkson, T. J. Price, and C. J. Adams, *J. Chem. Soc., Faraday Trans.* **88** (1992) 243–249.
88. J. M. Didymus, P. Oliver, S. Mann, A. L. DeVries, P. V. Hauschka, and P. Westbroek, *J. Chem. Soc., Faraday Trans.* **89** (1993) 2891–2900.
89. L. A. Gower and D. A. Tirrel, *J. Cryst. Growth* **191** (1998) 153–160.
90. S. K. Zang and K. E. Gonsalves, *Langmuir* **14** (1998) 6761–6766.
91. G. Xu, N. Yao, I. A. Aksay, and J. T. Goves, *J. Am. Chem. Soc.* **120** (1998) 11977–11985.
92. K. Naka, Y. Tanaka, Y. Chujo, and Y. Ito, *Chem. Commun.* (1999) 1931–1932.

93. J. Garcia-Carmona, J. Gómez-Morales, J. Fraile-Sainz, and R. Rodríguez-Clemente, *Powder Technol.* **130** (2003) 307–315.
94. G. Falini, S. Albeck, S. Weiner, and L. Addadi, *Science* **271** (1996) 67–69.
95. N. Wada, K. Yamasita, and T. Umegaki, *J. Colloid Interface Sci.* **212** (1999) 357–364.
96. A. M. Blecher, X. H. Wu, R. J. Christensen, P. K. Hansma, G. D. Stucky, and D. E. Morse, *Nature* **381** (1996) 56–58.
97. J. Aizenberg, J. Hanson, T. F. Koetzle, S. Weiner, and L. Addadi, *J. Am. Chem. Soc.* **119** (1997) 881–886.
98. P. Kaushansky and S. Yariv, *Appl. Geochem.* **1** (1986) 607–618.
99. S. L. Stipp and M. F. Hochella Jr., *Geochim. Cosmochim. Acta* **55** (1991) 1723–1736.
100. Lj. Brečević, V. Nöthig-Laslo, D. Kralj, and S. Popović, *J. Chem. Soc., Faraday Trans.* **92** (1996) 1017–1022.
101. J. Kushnir, *Geochim. Cosmochim. Acta* **44** (1980) 1471–1482.
102. R. B. Lorens, *Geochim. Cosmochim. Acta* **45** (1981) 553–561.
103. J. A. Davis, C. C. Fuller, and A. D. Cook, *Geochim. Cosmochim. Acta* **51** (1987) 1477–1490.
104. D. J. Kinsman and H. D. Holland, *Geochim. Cosmochim. Acta* **33** (1969) 1–17.
105. G. E. Barberis, R. Calvo, H. G. Maldonado, and C. E. Zarate, *Phys. Rev. B* **12** (1975) 853–860.
106. J. G. Angus, J. B. Raynor, and M. Robson, *Chem. Geol.* **27** (1979) 181–205.
107. V. Nothig-Laslo and Lj. Brečević, *J. Chem. Soc., Faraday Trans.* **94** (1998) 2005–2009.
108. V. Nöthig-Laslo and Lj. Brečević, *Phys. Chem. Chem. Phys.* **1** (1999) 3697–3700.
109. G. Falini, M. Gazzano, and A. Ripamonti, *J. Cryst. Growth* **137** (1994) 577–584.
110. F. C. Meldrum and S. T. Hyde, *J. Cryst. Growth* **231** (2001) 544–558.
111. G. Falini, M. Gazzano, and A. Ripamonti, *Chem. Commun.* (1996) 1037–1038.
112. K. J. Davis, P. M. Dove, and J. J. De Yereo, *Science* **290** (2000) 1134–1137.
113. F. Manoli and E. Dalas, *J. Cryst. Growth* **218** (2000) 359–364.
114. O. S. Pokrovsky, *J. Cryst. Growth* **186** (1998) 233–239.
115. H. Cölfen and L. Qi, *Chem. Eur. J.* **7** (2001) 106–116.
116. Y.-J. Han and J. Aizenberg, *J. Am. Chem. Soc.* **125** (2003) 4032–4033.
117. Y. Kitano, *Bull. Chem. Soc. Jpn.* **35** (1962) 1973–1980.
118. D. Kralj, J. Kontrec, Lj. Brečević, G. Falini, and V. Nöthig-Laslo, *Chem. Eur. J.* **10** (2004) 1647–1656.
119. J. Kontrec, D. Kralj, Lj. Brečević, G. Falini, S. Fermani, V. Nöthig-Laslo, and K. Miroslavljević, *Eur. J. Inorg. Chem.* (2004) 4579–4585.
120. M. M. Reddy, *J. Cryst. Growth* **41** (1977) 287–295.
121. R. G. Compton and C. A. Brown, *J. Colloid Interface Sci.* **16** (1994) 445–449.
122. I. Lebron and D. L. Suarez, *Geochim. Cosmochim. Acta* **60** (1996) 2765–2776.
123. L. Ji-Liang, R. M. Pytkowicz, *Chin. J. Oceanol. Limnol.* **6/4** (1988) 358–366.

---

## SAŽETAK

### O kalcijevim karbonatima: od osnovnih istraživanja do primjene

Ljerka Brečević i Damir Kralj

Pojavljivanje neke čvrste faze iz vodene otopine, poznato pod pojmom taloženje, odgovorno je za nastajanje brojnih prirodnih materijala i tehnoloških proizvoda. Zbog toga je, u područjima kao što su geologija, oceanologija, biomineralizacija, medicina, bazična kemijska i farmaceutska industrija, neophodno poznavanje mehanizama osnovnih procesa taloženja. Kalcijevi karbonati su veoma prikladan modelni sustav za istraživanje tih procesa. Zbog njihove niske topljivosti moguće je postići široki raspon početnih prezasićenosti sustava, što onda omogućuje uspostavljanje uvjeta pri kojima neki određeni proces prevladava. Kalcijevi se karbonati mogu javljati u šest različitih modifikacije (polimorfni i hidratni). U posljednjih su dvadesetak godina u Laboratoriju za procese taloženja provedena sistematska istraživanja uvjeta nastajanja, kristalnoga rasta i transformacije amornog kalcijeva karbonata, kalcijeva karbonata heksahidrata, kalcijeva karbonata monohidrata, vaterita i kalcita. Prikazan je pregled obavljenih istraživanja.